International Journal of Solids and Structures 49 (2012) 1241–1251

Contents lists available at SciVerse ScienceDirect

International Journal of Solids and Structures

journal homepage: www.elsevier.com/locate/ijsolstr

Stress intensity factors for an edge interface crack in a bonded semi-infinite plate for arbitrary material combination

Nao-Aki Noda *, Xin Lan

Department of Mechanical Engineering, Kyushu Institute of Technology, 1-1 Sensui-cho, Tobata-ku, Kitakyushu-shi, Fukuoka 804-8550, Japan

ARTICLE INFO

Article history:
Received 6 September 2011
Received in revised form 10 January 2012
Available online 10 February 2012

Keywords:
Stress intensity factor
Edge interface crack
Bonded semi-infinite plate
Material combination
Finite element method

ABSTRACT

Although a lot of interface crack problems were previously treated, few solutions are available under arbitrary crack lengths and material combinations. In this paper the stress intensity factors of an edge interface crack in a bonded strip are considered under tension with varying the crack length and material combinations systematically. Then, the limiting solutions are provided for an edge interface crack in a bonded semi-infinite plate under arbitrary material combinations. In order to calculate the stress intensity factors accurately, exact solutions in an infinite bonded plate are also considered to produce proportional singular stress fields in the analysis of FEM by superposing specific tensile and shear stresses at infinity. The details of this new numerical solution are described with clarifying the effect of the element size on the stress intensity factor. It is found that for the edge interface crack the normalized stress intensity factors are not always finite depending upon Dunders' parameters. This behavior can be explained from the condition of the singular stress at the end of bonded strip. Convenient formulas are also given by fitting the computed results.

1. Introduction

Modern technology has led to employing of composite structures in automotive and aerospace industries and multiple layers in microelectronics packaging. Failure of the multi-layer systems often initiates at the free-edge corner; therefore, the analysis of the edge interface crack is fundamental to our understanding of the initiation and propagation of free-edge cracks. An exhaustive investigation on the stress intensity factors (SIFs) will contribute better understanding of the initiation and propagation of the interfacial cracks.

Quite a lot interface crack problems have been treated previously, and various numerical methods have been reported to determine the SIFs of an interface crack till recently (Akisanya and Fleck, 1997; Dong et al., 1997; Liu et al., 2008; Wu, 1996; Xu et al., 1999; Yang and Kuang, 1996). However, several fundamental questions are still unsettled for interface cracks. For example, the equivalent condition is well-known for the SIFs between the central and edge interface cracks in homogenous wide plate in Fig. 1(a) and (b). Say, the stress intensity factor (SIF) of Fig. 1(b) is equivalent to $\sqrt{2} \times 1.1215$ times that of Fig. 1(a) when the two crack lengths are the same as $2a = a'$. On the other hand, for the interface cracks the similar equivalent condition has not been revealed yet for the SIFs between the central and edge interface cracks in the bonded dissimilar wide plates. In our previous studies, therefore, the central interface cracks in a dissimilar bonded plate in Fig. 1(c) have been treated under arbitrary material combinations (Noda et al., 2010; Zhang et al., 2011). In this study an edge interface cracks in bonded dissimilar semi-infinite plate will be considered as shown in Fig. 1(d), which is the most fundamental counterpart problem for interface cracks.

In this paper the SIFs at the crack tip in a bi-material bonded semi-infinite plate as shown in Fig. 1(d) will be investigated under arbitrary combination of materials. In order to calculate the stress intensity factors accurately, the exact solutions in an infinite bonded plate will be also considered to produce proportional singular stress fields by applying specific tensile and shear stresses at infinity. The details of this new numerical solution will be described with varying the minimum element size around the crack tip. The relationship between the SIF and the crack size in a bonded finite plate is discussed; then, finally an approximate formula for a shallow edge interface crack under arbitrary combination of materials and relative crack size will be given by fitting the computed results.

2. Analysis method

2.1. The physical background

Teranisi and Nisitani (1999) were the first to propose a numerical method using FE stress values to compute the SIF of a cracked

* Corresponding author.
E-mail address: noda@mech.kyutech.ac.jp (N.-A. Noda).

0020-7683/$ - see front matter © 2012 Elsevier Ltd. All rights reserved.
doi:10.1016/j.ijsolstr.2012.02.001

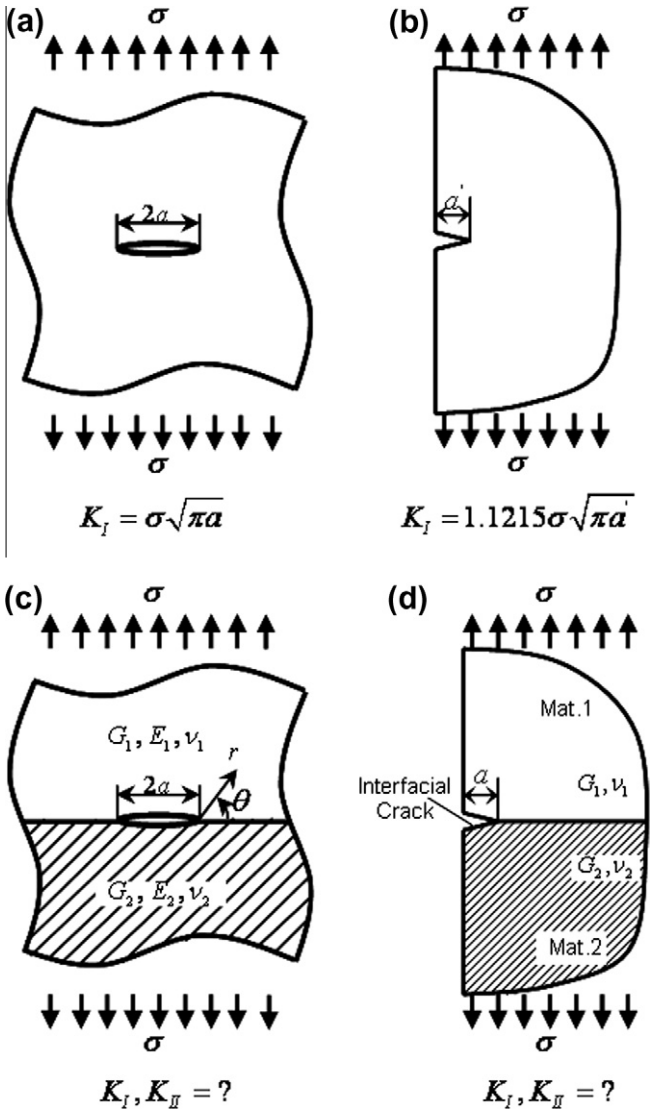

Fig. 1. (a) Center cracked and (b) edge cracked homogenous wide plate (c) center cracked and (d) edge cracked dissimilar bonded wide plate.

homogenous plate. According to the theory of linear-elastic fracture mechanics (LEFM), mode I SIF near the crack tip in a homogenous plate is defined by the following equation.

$$\sigma_{yy}(r,\theta) \to \frac{K_I}{\sqrt{2\pi r}} f_I(\theta) \quad (r \to 0) \tag{1}$$

Here, K_I is the mode I SIF, σ_{yy} is the normal stress component ahead of the crack tip, $f_I(\theta)$ is trigonometric function to be derived analytically. Specifically, when $\theta = 0$, Eq. (1) becomes

$$\sigma_y(r) \to \frac{K_I}{\sqrt{2\pi r}}, \quad \sigma_y = \sigma_{yy}|_{\theta=0} \ (r \to 0) \tag{2}$$

Rearranging Eq. (2) gives $K_I/\sigma_y \to \sqrt{2\pi r}$ $(r \to 0)$. For a given point at $\theta = 0$ with a distance from the crack tip $r = r_0$, $K_I/\sigma_y = \sqrt{2\pi r_0}$ is constant and a following relationship can be deduced theoretically for two different crack problems A and B

$$[K_I^*/\sigma_y^*]_A = [K_I/\sigma_y]_B \tag{3}$$

Assuming the SIF for problem A is analytically given in advance, while that for problem B is yet to be solved. Problem A is denoted as the reference problem and problem B is denoted by the given unknown problem. Here, the superscript $*$ is introduced to indicate the values of the reference problem A for notational convenience. Although the values of σ_y^*, σ_y in Eq. (3) cannot be computed by FE analysis easily, the ratio of the value can be given without difficulty. This is because the error for the problems A and B are nearly the same if the same FE mesh is applied to the problems A and B

$$\frac{[K_I]_B}{[K_I^*]_A} = \frac{[\sigma_y]_B}{[\sigma_y^*]_A} = \frac{[\sigma_{y,FEM}]_B}{[\sigma_{y,FEM}^*]_A} \quad \text{although} \quad [\sigma_y]_B \neq [\sigma_{y,FEM}]_B \tag{4a}$$

It has been reported by Teranisi and Nisitani (1999) that the stress distributions computed by FEM are almost the same under the same loading conditions of $K_I = const$ for various crack problems, independent of the crack lengths. Then the SIF for problem B (the given unknown problem) can be accurately determined using Eq. (4). It should be noted that the same FE mesh grids have to be used in the singular region near the crack tip to compute σ_y^*, σ_y for the two different crack problems A and B

$$[K_I]_B = \frac{[\sigma_{y,FEM}]_B}{[\sigma_{y,FEM}^*]_A}[K_I^*]_A \tag{4b}$$

2.2. Formulation for the interface crack problems

The method discussed in Section 2.1 cannot be used directly into solving the interface crack problems since oscillatory singularity is observed along the interface. Oda et al., 2009, extended this method to the interface crack problems by creating the same singularities for the reference and given unknown problems. A definition of the SIFs for an interface crack in bonded dissimilar materials was proposed by Erdogan, 1965. The stress distributions along the interface are defined as shown in Eq. (5)

$$\sigma_y + i\tau_{xy} = \frac{K_I + iK_{II}}{\sqrt{2\pi r}}\left(\frac{r}{2a}\right)^{i\varepsilon}, \quad r \to 0 \tag{5}$$

Here, σ_y, τ_{xy} denote the stress components near the crack tip, r is the radial distance from the crack tip, and ε is the bi-elastic constant given by:

$$\varepsilon = \frac{1}{2\pi}\ln\left[\left(\frac{\kappa_1}{G_1} + \frac{1}{G_2}\right)\Big/\left(\frac{\kappa_2}{G_2} + \frac{1}{G_1}\right)\right] \tag{6}$$

$$\kappa_m = \begin{cases} 3 - 4\nu_m & (\textit{plane strain}), \\ 3 - \nu_m/1 + \nu_m & (\textit{plane stress}), \end{cases} \quad (m = 1,2) \tag{7}$$

Where G_m $(m = 1,2)$ and ν_m $(m = 1,2)$ are the shear moduli and Poisson's ratios of either respective materials. The real and imaginary parts of the oscillatory SIFs $K_I + iK_{II}$ in Eq. (5) may be separated as

$$K_I = \lim_{r\to 0}\sqrt{2\pi r}\sigma_y\left(\cos Q + \frac{\tau_{xy}}{\sigma_y}\sin Q\right) \tag{8}$$

$$K_{II} = \lim_{r\to 0}\sqrt{2\pi r}\tau_{xy}\left(\cos Q + \frac{\sigma_y}{\tau_{xy}}\sin Q\right) \tag{9}$$

and

$$Q = \varepsilon\ln\left(\frac{r}{2a}\right) \tag{10}$$

Similarly, let us consider two different interface crack problems C and D with the same crack lengths $a = a_0$ and the same combination of materials $\varepsilon = \varepsilon_0$, assuming the SIFs of problem C are given in advance and those for problem D are yet to be solved. Problem C is termed the reference problem whose values are marked with $*$, and problem D is termed the given unknown problem. Examining the points with the same radial distances $r = r_0$ for the two

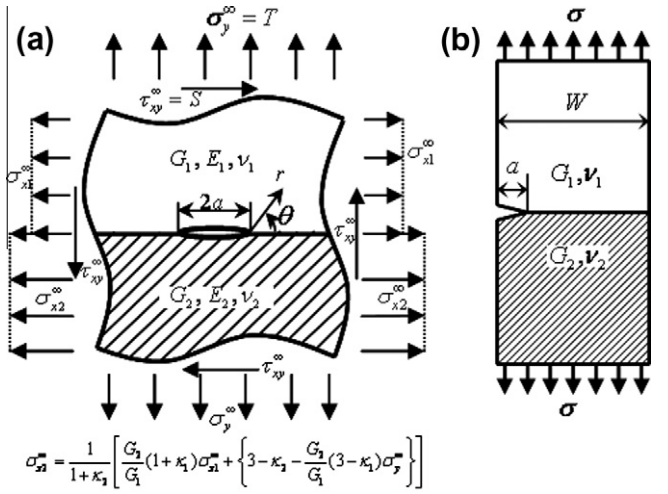

Fig. 2. Demonstration of (a) the reference problem (problem C) and (b) a given unknown problem (problem D).

problems C and D, then gives $[Q^*]_C = [Q]_D = \varepsilon_0 \ln(\frac{r_0}{2a_0})$. Recall Eqs. (8) and (9), a proportional relationship given in Eq. (11) is established if and only if Eq. (12) can be satisfied,

$$\frac{[K_I]_D}{[K_I^*]_C} = \frac{[\sigma_y]_D}{[\sigma_y^*]_C} = \frac{[\sigma_{y,FEM}]_D}{[\sigma_{y,FEM}^*]_C}, \quad \frac{[K_{II}]_D}{[K_{II}^*]_C} = \frac{[\tau_{xy}]_D}{[\tau_{xy}^*]_C} = \frac{[\tau_{xy,FEM}]_D}{[\tau_{xy,FEM}^*]_C} \tag{11}$$

$$\left[\frac{\tau_{xy}^*}{\sigma_y^*}\right]_C = \left[\frac{\tau_{xy}}{\sigma_y}\right]_D \tag{12}$$

Then the SIFs of the given unknown problem (problem D) can be computed using Eq. (13) in a similar manner as discussed in Section 2.1. The condition of Eq. (12) can be satisfied by choosing a suitable external load for the reference problem. The detailed information about how to make the condition Eq. (12) satisfied by using FEM will be discussed in Section 2.3

$$\begin{aligned}[K_I]_D &= \frac{[\sigma_y]_D[K_1^*]_C}{[\sigma_y^*]_C} = \frac{[\sigma_{y,FEM}]_D[K_1^*]_C}{[\sigma_{y,FEM}^*]_C},\\ [K_{II}]_D &= \frac{[\tau_{xy}]_D[K_2^*]_C}{[\tau_{xy}^*]_C} = \frac{[\tau_{xy,FEM}]_D[K_2^*]_C}{[\tau_{xy,FEM}^*]_C}\end{aligned} \tag{13}$$

2.3. Application of the proportional method using FEM

In this research, a crack along the interface of two bonded dissimilar half-planes subjected to tension and shear as shown in Fig. 2(a) is treated as the reference problem. The analytical solution of the SIFs at the crack tip for the reference problem takes the form

$$K_I^* + iK_{II}^* = (\sigma_y^\infty + i\tau_{xy}^\infty)\sqrt{\pi a}(1 + 2i\varepsilon) \tag{14}$$

where σ_y^∞, τ_{xy}^∞ are the remote uniform tension and shear applied to the bonded dissimilar half-planes.

Using the principle of superposition, the stress components of the reference problem subject to remote tension and shear σ_y^∞, τ_{xy}^∞ can be expressed by using the values of that subjected to pure unite tension $\sigma_y^\infty = 1$, $\tau_{xy}^\infty = 0$ and pure unite shear $\sigma_y^\infty = 0$, $\tau_{xy}^\infty = 1$. Let $\sigma_{y0,FEM}^*$, $\tau_{xy0,FEM}^*$, $\sigma_{y0,FEM}^{\sigma_y^\infty=1,\tau_{xy}^\infty=0*}$, $\tau_{xy0,FEM}^{\sigma_y^\infty=1,\tau_{xy}^\infty=0*}$ and $\sigma_{y0,FEM}^{\sigma_y^\infty=0,\tau_{xy}^\infty=1*}$, $\tau_{xy0,FEM}^{\sigma_y^\infty=0,\tau_{xy}^\infty=1*}$ denote the stress components at the crack tip of the reference problem subjected to combined remote tension and shear σ_y^∞, τ_{xy}^∞, pure unit tension $\sigma_y^\infty = 1$, $\tau_{xy}^\infty = 0$ and pure unit shear $\sigma_y^\infty = 0, \tau_{xy}^\infty = 1$, respectively. Then $\sigma_{y0,FEM}^*$, $\tau_{xy0,FEM}^*$ take the form

$$\sigma_{y0,FEM}^* = \sigma_{y0,FEM}^{\sigma_y^\infty=1,\tau_{xy}^\infty=0*} \times \sigma_y^\infty + \sigma_{y0,FEM}^{\sigma_y^\infty=0,\tau_{xy}^\infty=1*} \times \tau_{xy}^\infty \tag{15}$$

$$\tau_{xy0,FEM}^* = \tau_{xy0,FEM}^{\sigma_y^\infty=1,\tau_{xy}^\infty=0*} \times \sigma_y^\infty + \tau_{xy0,FEM}^{\sigma_y^\infty=0,\tau_{xy}^\infty=1*} \times \tau_{xy}^\infty \tag{16}$$

Recall Eq. (12), the FE stress components at the crack tip for the problems C and D behave

$$\left[\frac{\tau_{xy0,FEM}^*}{\sigma_{y0,FEM}^*}\right]_C = \left[\frac{\tau_{xy0,FEM}}{\sigma_{y0,FEM}}\right]_D \tag{17}$$

where the superscript 0 stands for the values at the crack tip. Inserting Eqs. (15) and (16) into Eq. (17) gives the solution of $\tau_{xy}^\infty/\sigma_y^\infty$ needed for determining the external loads applied to the reference problem

$$\frac{\tau_{xy}^\infty}{\sigma_y^\infty} = \frac{\sigma_{y0,FEM} \times \tau_{xy0,FEM}^{\sigma_y^\infty=1,\tau_{xy}^\infty=0*} - \tau_{xy0,FEM} \times \sigma_{y0,FEM}^{\sigma_y^\infty=1,\tau_{xy}^\infty=0} *}{\tau_{xy0,FEM} \times \sigma_{y0,FEM}^{\sigma_y^\infty=0,\tau_{xy}^\infty=1*} - \sigma_{y0,FEM} \times \tau_{xy0,FEM}^{\sigma_y^\infty=0,\tau_{xy}^\infty=1*}} \tag{18}$$

Let $\sigma_y^\infty \infty = 1$ so that τ_{xy}^∞ can be determined. Inserting $\sigma_y^\infty = 1, \tau_{xy}^\infty$ into Eq. (14) gives the values of the oscillatory SIFs for the reference problem (problem C). Finally, the SIFs for the given unknown problem (problem D) can be yielded using the proportional relationship as given in Eq. (19)

$$[K_I]_D = \frac{[\sigma_{y0,FEM}]_D[K_I^*]_C}{[\sigma_{y0,FEM}^*]_C}, \quad [K_{II}]_D = \frac{[\tau_{xy0,FEM}]_D[K_{II}^*]_C}{[\tau_{xy0,FEM}^*]_C} \tag{19}$$

Specially, when both materials for a bonded structure are identical, all the imaginary terms in the discussion vanish. Thus, the current method is also applicable to the homogenous crack problems.

3. Post-processing technique and Convergence study

According to Oda et al., 2009, the proportional method does not give reliable results if the relative crack size is considerably deep (say, $a/W \geqslant 0.4$). Then, the efficiency and accuracy of the proportional method is demonstrated by pursuing a convergence study in this research. The effects of the minimum element size e and the number of refined layers NL around the singular region on the mode I SIF values are discussed. Finally, a post-processing technique of linear extrapolation is proposed to improve the accuracy. The finite element analysis package MSC.MARC 2007 r1 (2007) is used in this research. It is concluded that exact SIFs can be obtained using linear extrapolation.

Two-dimensional plane-stress problem of a single-edge cracked bonded dissimilar strip is analyzed for various crack lengths (for a range of $a/W = 0.1 \sim 0.9$). The geometric configurations for the given unknown and reference problems are shown in Fig. 3(a) and (b), respectively. The four-node quadrilateral elements are used to mesh the reference and the given unknown problems. Fig. 4 shows the mesh type for a single-edge cracked strip (the given unknown problem). The singular region around the crack tip is well refined with increasing numbers of layers. The element size for each inferior layer is one third of that of the superior one. And the meshes for the reference problem are subdivided in a self-similar manner as shown in Fig. 4. It should be noted that the meshes around the singular zone for the reference and given unknown problems are kept the same, then, the FE computational errors will be eliminated in the proportional process. Here, four pairs of models (the reference + the given unknown problems) with different minimum element sizes are tested to carry out the convergence study. The minimum element size for each pair of models is $a/3^5$, $a/3^6$, $a/3^7$, $a/3^8$ which corresponds to the total number of layers $NL = 9$, 10, 11, 12 respectively. The detailed measurements for the FE models are tabulated in Table 1. The length L is assumed

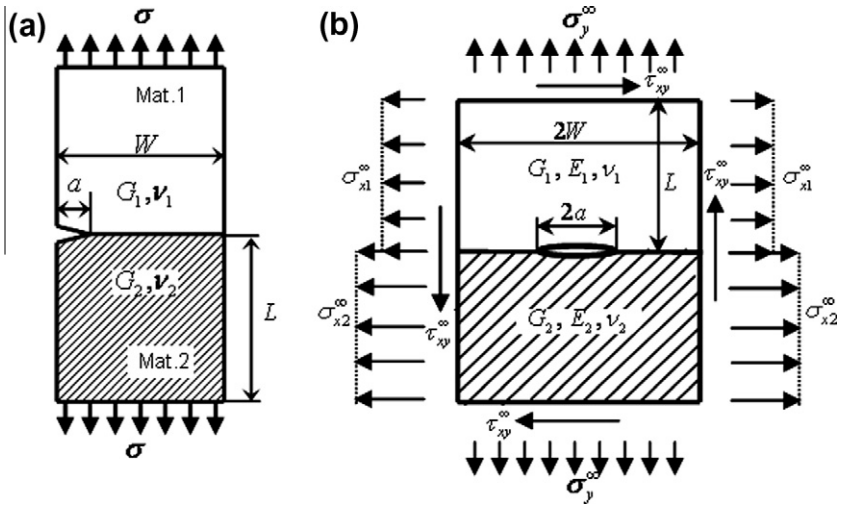

Fig. 3. FEM model geometric configurations for (a) the given unknown problem and (b) the reference problem.

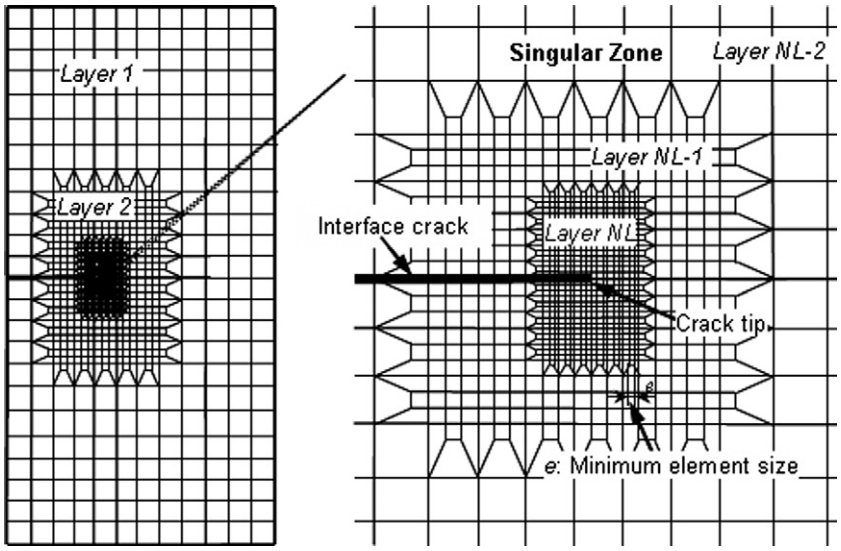

Fig. 4. FEM mesh demonstration of the geometry of a single edge-cracked strip.

Table 1
Measurements for the FE models.

	The reference problem (mm)				The given unknown problem (mm)			
	Case 1	Case 2	Case 3	Case 4	Case 1	Case 2	Case 3	Case 4
a	10	10	10	10	10	10	10	10
a/*W*	1/1620	1/1620	1/1620	1/1620	0.1∼0.9	0.1∼0.9	0.1∼0.9	0.1∼0.9
e	10/243	10/729	10/2187	10/6561	10/243	10/729	10/2187	10/6561
NL	9	10	11	12	–	–	–	–

a: crack length of an edge crack or half crack length of a central crack *a*/*W*: relative crack length. *W* denotes the width of the plate. *e*: minimum element size around a crack tip *NL*: number of the refined layers for the reference problem.

to be much greater than the width W ($L = 2W$ is used in the FE model).

In the analysis, the elastic parameters are restricted to $G_2/G_1 = 4$, $v_2 = v_1 = 0.3$. The SIFs for the edge cracked dissimilar bonded strip $a/W = 0.7, 0.8$ are plotted and compared with those of Yuuki and Cho (1989) and Ikeda et al. (1993), in Fig. 5. Those of others' data are plotted in dashed lines. From this figure, it can be seen that the normalized SIFs $K_I/\sigma\sqrt{\pi a}$ behave linear relationship with the minimum element size. Final results can be obtained by using linear extrapolation without adding too more refined layers. Here, it should be noted that the exact values for $K_{II}/\sigma\sqrt{\pi a}$ are computed through extrapolation although a simple linear behavior is not observed for the last fourth digit. Also for no deep crack, post-processing of extrapolation is applied since the effect of minimum element size e to the SIFs is dominated. This means the original method may include un-ignored error for the not deep crack case. According to the authors' knowledge, the minimum element size $e = a/3^5, a/3^6$ may be recommended for the extrapolation since

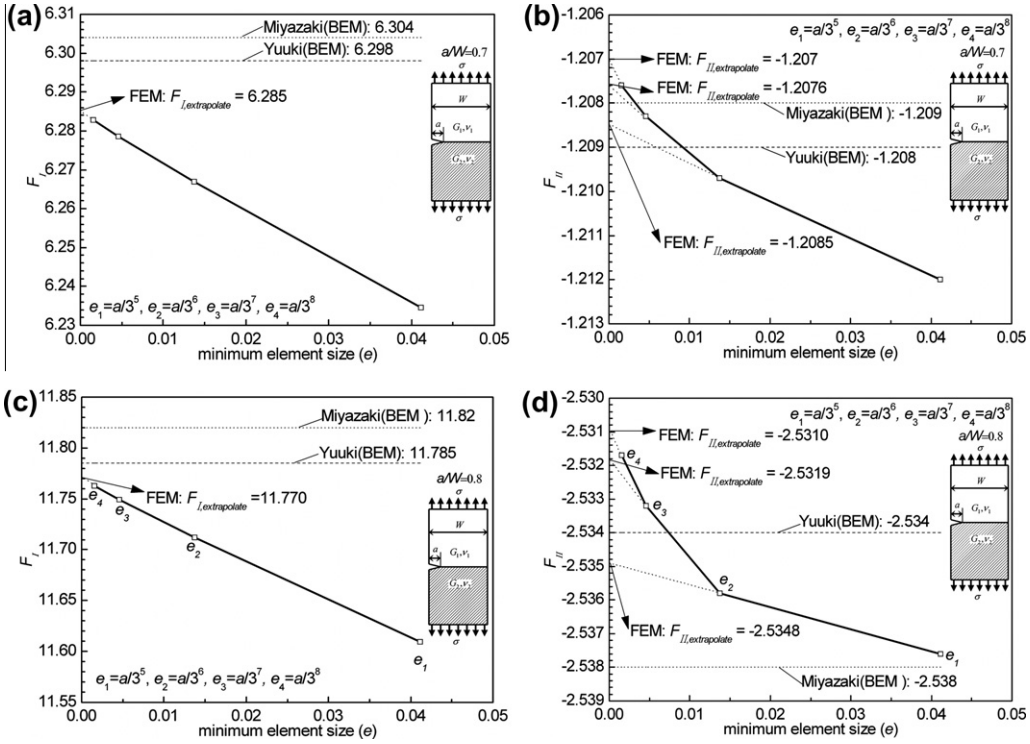

Fig. 5. Variations of normalized SIFs $F_I = K_I/\sigma\sqrt{\pi a}, F_{II} = K_{II}/\sigma\sqrt{\pi a}$ with the minimum element size e for a bonded strip (a) $a/W = 0.7$ and (b) $a/W = 0.8$ subjected to uniform tension.

Table 2
Normalized stress intensity factors for Fig. 2(b) ($G_2/G_1 = 4$, $\upsilon_1 = \upsilon_2 = 0.3$, plane stress).

a/W	$K_I/\sigma\sqrt{\pi a}$				$K_{II}/\sigma\sqrt{\pi a}$			
	Present	Oda et al. (2009)	Yuuki and Cho (1989)	Ikeda et al. (1993)	Present	Oda et al. (2009)	Yuuki and Cho (1989)	Ikeda et al. (1993)
0.1	1.209	1.207	1.201	1.209	−0.2393	−0.240	−0.238	−0.239
0.2	1.368	1.365	1.387	1.368	−0.250	−0.251	−0.254	−0.250
0.3	1.653	1.644	1.653	1.654	−0.288	−0.286	−0.288	−0.288
0.4	2.100	2.093	2.100	2.101	−0.359	−0.359	−0.359	−0.359
0.5	2.805	2.791	2.807	2.807	−0.484	−0.484	−0.483	−0.483
0.6	3.998	–	4.000	4.006	−0.716	–	−0.716	−0.716
0.7	6.285	–	6.298	6.304	−1.207	–	−1.209	−1.208
0.8	11.770	–	11.785	11.82	−2.532	–	−2.534	−2.538
0.9	33.746	–	–	–	−8.792	–	–	–

they have the best compromise between accuracy and computational cost. It should be noted that the SIFs are almost constant and independent of the minimum element size for central cracks even in the case of long crack differently from Fig. 5.

The normalized SIFs are tabulated in Table 2 together with those of Yuuki and Cho (1989) and Ikeda et al. (1993). Table 2 illustrates that the results are in very good agreement with the present results. The errors are within 0.13% for mode I and 0.03 for mode II for $a/W = 0.8$. Thus, the results computed by the current method are much better than those by the original one especially for the deep crack. Furthermore, the current method can get the accurate SIFs without using too many layers of refined meshes (say, the total number of layers is $NL = 9$, 10 in this research), and it has a faster convergence than other numerical methods.

4. Relationship between the stress intensity factors and crack length

Consider the bi-material bonded plate shown in Fig. 1(d). It is composed of two elastic, isotropic and homogeneous semi-infinite plates that are perfectly bonded along the interface. The material above the interface is termed material 1, and the material below is termed material 2. The SIFs for the aforementioned problem in plane strain or plane stress are only determined on the two elastic mismatch parameters α and β (Dundurs, 1969). Here, the Dundurs' material composite parameters are defined as

$$\alpha = \frac{G_1(\kappa_2+1) - G_2(\kappa_1+1)}{G_1(\kappa_2+1) + G_2(\kappa_1+1)} \tag{20}$$

$$\beta = \frac{G_1(\kappa_2-1) - G_2(\kappa_1-1)}{G_1(\kappa_2+1) + G_2(\kappa_1+1)} \tag{21}$$

where the subscripts denote material 1 or 2, $G_m = E_m/2(1+\nu_m)$ $(m = 1, 2)$, G_m, E_m and ν_m denote shear modulus, Young's modulus and Poisson's ratio for material m, respectively. $\kappa_m = (3-\nu_m)/(1+\nu_m)$ for plane stress and $\kappa_m = (3-4\nu_m)$ for plane strain. In this research, only the SIFs for $\beta \geqslant 0$ in $\alpha - \beta$ space has been investigated since switching material 1 and 2 ($mat1 \Longleftrightarrow mat2$) will only reverse the signs of α and β ($(\alpha, \beta) \Longleftrightarrow (-\alpha, -\beta)$).

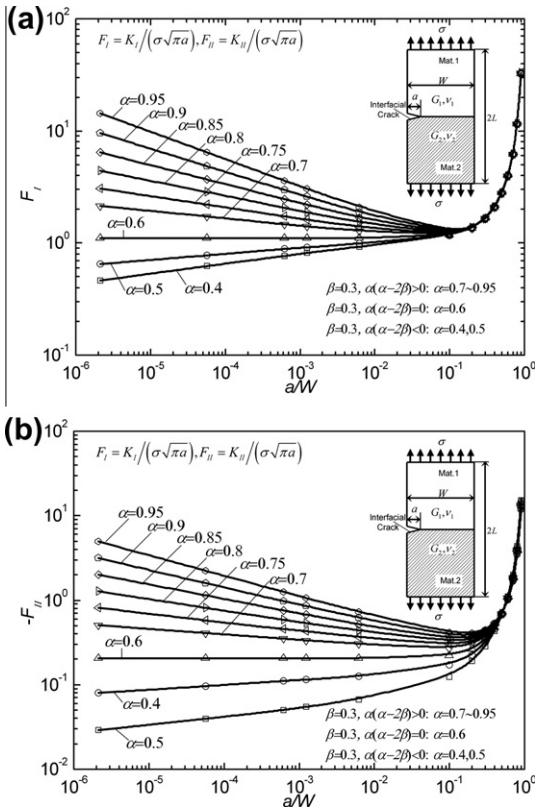

Fig. 6. The double logarithmic distributions of the dimensionless stress intensity factors (a) $F_I = K_I/\sigma\sqrt{\pi a}$ and (b) $F_{II} = K_{II}/\sigma\sqrt{\pi a}$ at the crack tip for shallow edge interface cracks.

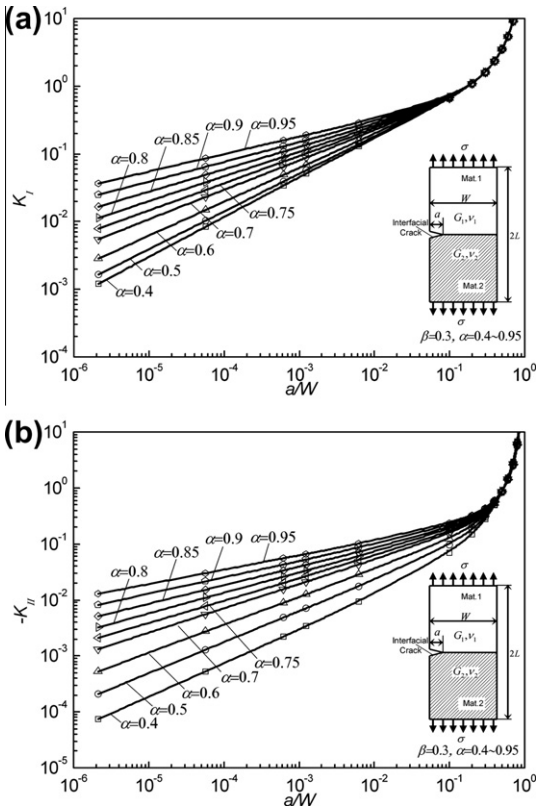

Fig. 7. The double logarithmic distributions of the general SIFs K_I and K_{II} at the crack tip for shallow edge interface cracks.

The normalized SIFs at the crack tip of the edge interface crack in bi-material bonded strips are systematically investigated by varying the relative crack size *a*/*W*, as well as the material elastic parameters α and β. Here, we restrict our discussion to material combinations with $\beta = 0.3$because the same phenomenon can be found from others material combinations. The double logarithmic distributions are shown in Fig. 6(a) and (b) for the normalized SIFs $F_I = K_I/\sigma\sqrt{\pi a}$, $F_{II} = K_{II}/\sigma\sqrt{\pi a}$, respectively. From those figures, it is found that the double logarithmic distributions behave linearity when $a/W < 0.01$ and differ within about 5% at $a/W < 0.05$.

Furthermore, after examining every material combination, it is found that the plus and minus of the slope of each curve is always controlled by the sign of $\alpha(\alpha - 2\beta)$. The value of the slope is equivalent to the order of stress singularity at the interfacial end of a perfectly bonded strip. Specifically, the slope of each line is positive when $\alpha(\alpha - 2\beta) < 0$, zero when $\alpha(\alpha - 2\beta) = 0$ and is negative when $\alpha(\alpha - 2\beta) > 0$. This is known as the condition of existence of free edge stress singularity at the interfacial end. For example, free-edge singularity exists when the slope is negative and vanishes when it is positive. In particular, uniform stress distribution appears when the slope is 0. The values of α, β are discussed in the appendix for typical engineering materials (Yuuki, 1992). Thus, it can also be deduced for the limiting case, the values of $F_I = K_I/\sigma\sqrt{\pi a}$, $F_{II} = K_{II}/\sigma\sqrt{\pi a}$ for the bonded semi-infinite plate ($a/W \to 0$) take the form:

$$\begin{aligned} &\alpha(\alpha-2\beta) > 0: \quad F_I, F_{II} \to \infty \\ &\alpha(\alpha-2\beta) = 0: \quad F_I, F_{II} \to \text{finite} \\ &\alpha(\alpha-2\beta) < 0: \quad F_I, F_{II} \to 0 \end{aligned} \tag{22}$$

Although when $\alpha(\alpha - 2\beta) > 0$ $F_I \to \infty$ and $F_{II} \to \infty$ as $a/W \to 0$, actual crack extension along the interface may be controlled by the stress intensity factors K_I, K_{II} instead of F_I, F_{II}. In order to simulate the crack extension it is important to consider how the values of K_I, K_{II} change depending on the crack length. The double logarithmic distributions of the general SIFs K_I and K_{II} at the crack tip are plotted in Fig. 7. A good linear relationship within the zone of the free-edge singularity can also be found from this figure. Here, it should be noted that all the SIFs increase monotonically with increasing relative crack length a/W for all the material combinations. Since F_I, F_{II} sometimes go to infinity, one may misunder-

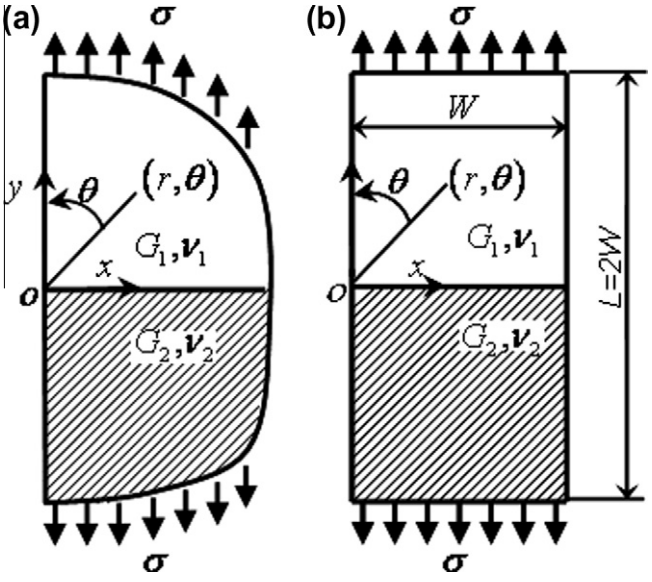

Fig. 8. (a) The bi-material bonded semi-infinite plate and (b) finite strip.

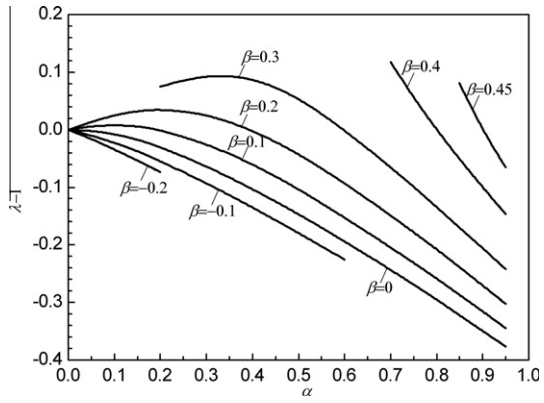

Fig. 9. Order of stress singularity $\lambda - 1$.

stand that K_I, K_{II} also approach infinity as $a/W \to 0$. However, as shown in Fig. 7, it is seen that K_I, K_{II} always approach zero independent of material combinations as $a/W \to 0$.

5. Singular stress field at the end of bonded plate

As shown in the previous section, the stress intensity factor of an edge interface crack may be affected by the singular stress field appearing at the end of bonded plate. It should be noted that more detail investigation reveals that the slopes of $F_I = K_I/\sigma\sqrt{\pi a}$, $F_{II} = K_{II}/\sigma\sqrt{\pi a}$ in Fig. 6 correspond to the singular index λ at the end of bonded plate without crack. It is known that this singularity at the end of bonded plate can be determined by the following relationships (Bogy, 1968, 1971)

$$\begin{aligned}
&\alpha(\alpha-2\beta)>0:\lambda<1, \quad \sigma_y=\sigma_{yy}|_{\theta=0}\to\infty \quad (r\to 0) \quad \text{Singularity exist}\\
&\alpha(\alpha-2\beta)=0:\lambda=1\sigma_y=\sigma_{yy}|_{\theta=0}\to \textit{finite} \quad (r\to 0) \quad \text{Singularity}=0\\
&\alpha(\alpha-2\beta)<0:\lambda>1\sigma_y=\sigma_{yy}|_{\theta=0}\to 0 \quad (r\to 0) \quad \text{Singularity vanish}
\end{aligned} \tag{23}$$

As a result, the interface crack within this zone behaves in the following ways

$$\alpha(\alpha-2\beta)>0;\ K_I/\sigma\sqrt{\pi a}\to\infty, \quad K_{II}/\sigma\sqrt{\pi a}\to\infty,$$

$$\alpha(\alpha-2\beta)=0;\ K_I/\sigma\sqrt{\pi a}, \quad K_{II}/\sigma\sqrt{\pi a}\to \text{finite values}$$

$$\alpha(\alpha-2\beta)<0;\ K_I/\sigma\sqrt{\pi a}\to 0, \quad K_{II}/\sigma\sqrt{\pi a}\to 0$$

In this section, the singular stress fields near the free-edge corner are described in detail because they control the interface crack within the singular zone. Let us consider a perfectly bonded dissimilar plate without crack as shown in Fig. 8 with a cylindrical polar coordinate (r,θ) centered at the interface corner. The singular field around the bonded end can be expressed in the form (Chen and Nishitani, 1993).

$$\sigma_\theta = Kr^{\lambda-1}f_{\theta\theta}(r,\theta), \quad \tau_{r\theta} = Kr^{\lambda-1}f_{r\theta}(r,\theta) \tag{24}$$

Here K is the intensity of stress singularity at bonded corner, r is the radial distance from the corner, and λ is the order of stress singularity. Also $f_{\theta\theta}(r,\theta)$, $f_{r\theta}(r,\theta)$ are known functions of r, θ given in Chen and Nishitani, 1993.

Many studies have considered the order of the stress singularity for bonded corners with varying geometries and material combinations (see, Williams, 1952; Bogy, 1968, 1971; Bogy and Wang, 1971; Hein and Erdogan, 1971; Dempsey and Sinclair, 1979; Van Vroonhoven, 1992). For the bonded strip shown in Fig. 8, the angles which the traction-free surfaces make with the interface are $\pi/2$, then the values of λ can be obtained by solving the following equation

$$\begin{aligned}
\mathrm{D}(\alpha,\beta,\lambda) = &\left[\cos^2\left(\frac{\pi}{2}\lambda\right)-(1-\lambda)^2\right]^2\beta^2\\
&+2(1-\lambda)^2\left[\cos^2\left(\frac{\pi}{2}\lambda\right)-(1-\lambda)^2\right]\alpha\beta\\
&+(1-\lambda)^2[(1-\lambda)^2-1]\alpha^2+\cos^2\left(\frac{\lambda\pi}{2}\right)\sin^2\left(\frac{\lambda\pi}{2}\right)=0
\end{aligned} \tag{25}$$

where λ is the zero of $\mathrm{D}(\alpha,\beta,\lambda)$ in $0<\mathrm{Re}(\lambda)<1$ that has the smallest real part. In general, $\mathrm{D}(\alpha,\beta,\lambda)$ is expected to have several zeros in $0<\mathrm{Re}(\lambda)<1$. In all cases where more than one zero of $\mathrm{D}(\alpha,\beta,\lambda)$ occurs only the smallest one will be exhibited (Bogy, 1971). The values of λ are computed for arbitrary material composite parameters (α,β), and the results are plotted and tabulated in Fig. 9 and in Table 3, respectively. Here, it should be noticed that λ for any material combination can be obtained from Table 6 since $\lambda(\alpha,\beta)=\lambda(-\alpha,-\beta)$.

Although the singular index has been discussed in many papers, the intensity of singular stress fields has just recently been obtained. Reedy and Guess, 1993 have determined the magnitude of intensity of stress singularity for a thin elastic layer sandwiched between two rigid substrates. Akisanya and Fleck (1997), applied the contour integral to evaluate the singular stress field at the free-edge of a long bi-material strip subjected to uniform tension. Xu et al. (1999) proposed numerical methods to determine the multiple stress singularities and the related stress intensity coefficients. Chen and Nishitani obtained the exact expression of the singular stress field for a bonded dissimilar strip. From this paper, it is known that the root of Eq. (25) has a single real root $0<\lambda<1$

Table 3
Singular index λ for various combination of materials.

α	$\beta=-0.2$	$\beta=-0.1$	$\beta=0$	$\beta=0.1$	$\beta=0.2$	$\beta=0.3$	$\beta=0.4$	$\beta=0.45$
0	1	1	1	1	1			
0.05	0.98378	0.99035	0.99800	1.00613	1.01403			
0.1	0.96593	0.97774	0.99205	1.00831	1.02512			
0.15	0.94684	0.96269	0.98253	1.00626	1.03279			
0.2	0.92685	0.94571	0.96987	1	1.03604	1.07562		
0.3		0.90752	0.93713	0.97605	1.02764	1.09640		
0.4		0.86549	0.89741	0.94025	1	1.09130		
0.5		0.82096	0.85320	0.89662	0.95796	1.05584		
0.6		0.77459	0.80597	0.84801	0.90711	1		
0.7			0.75644	0.79606	0.85104	0.93477	1.11741	
0.75			0.73090	0.76909	0.82169	0.90048	1.05468	
0.8			0.70481	0.74151	0.79163	0.86554	1	
0.85			0.67824	0.71331	0.76091	0.83006	0.94923	1.08125
0.9			0.65105	0.68448	0.72953	0.79410	0.90075	1
0.95			0.62320	0.65496	0.69745	0.75761	0.85364	0.93488
1			0.59461	0.62466	0.66461	0.72053	0.80731	0.87624

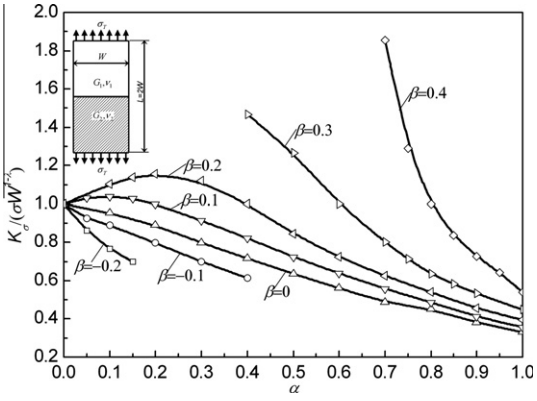

Fig. 10. The values of $K_\sigma/\sigma W^{1-\lambda}$ for various combination of materials.

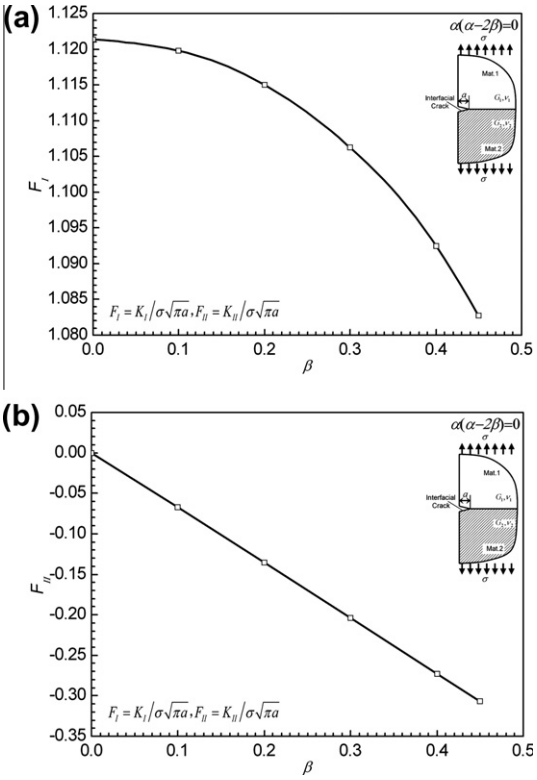

Fig. 11. Normalized SIFs (a) $F_I = K_I/\sigma\sqrt{\pi a}$ and (b) $F_{II} = K_{II}/\sigma\sqrt{\pi a}$ for $\alpha = 2\beta$ of an edge interface crack in a bonded semi-infinite plate.

when $\alpha(\alpha - 2\beta) > 0$. In this research, in order to examine the stress field around the free-edge corner, K_σ is introduced to define the intensity of singular stress as

$$K_\sigma = \lim_{r\to 0}[r^{1-\lambda} \times \sigma_{\theta|\theta=\pi/2}] \tag{26}$$

The intensity of stress singularity K for an un-cracked bonded dissimilar strip can be obtained using (Chen and Nishitani, 1993).

$$K = K_\sigma/(4\lambda\cos(\lambda\pi/2)[(\lambda+1-\lambda\beta)\cos(\lambda\pi) + (\lambda+1)(2\lambda\beta - 1) - \lambda\beta + 2\lambda^2(\lambda+1)(\alpha-\beta)]) \tag{27}$$

As a supplementary work to the authors' previous research (Noda et al., 2007), the normalized values of $K_\sigma/\sigma W^{1-\lambda}$ for $\lambda > 1$ are computed in this paper, and are plotted in Fig. 10 against material composite parameters α for $\beta = -0.2 \sim 0.4$.

Table 4
Results of the dimensionless stress intensity factors for $\alpha = 2\beta$.

β	$K_I/\sigma\sqrt{\pi a}$	$K_{II}/\sigma\sqrt{\pi a}$
0	1.121	0
0.1	1.120	−0.067
0.2	1.115	−0.135
0.3	1.106	−0.204
0.4	1.092	−0.273
0.45	1.083	−0.307

6. Stress intensity factors for the edge interface crack in a bonded semi-infinite plate

6.1. Approximate expressions for the stress intensity factors of a bonded semi-infinite plate

In Section 4, it has been proved that $K_I/\sigma\sqrt{\pi a}$ and $K_{II}/\sigma\sqrt{\pi a}$ have finite non-zero values only when $\alpha(\alpha - 2\beta) = 0$. Here, the normalized SIFs $F_I = K_I/\sigma\sqrt{\pi a}$ and $F_{II} = K_{II}/\sigma\sqrt{\pi a}$ for an edge interface crack in a bonded semi-infinite plate for $\alpha = 2\beta$ are plotted in Fig. 11. From the figure, it is clear that F_I and F_{II} behave quadratic and linear relationship, respectively. The computed results for $\alpha = 2\beta$ are also tabulated in Table 4. Then, the approximate expression as in Eq. (28) is given by fitting the computed results. Specifically, the result for the homogenous semi-infinite plate (when two materials are identical $\alpha = \beta = 0$) computed in this research is $K_I/\sigma\sqrt{\pi a} = 1.1208$, compared with the famous theoretical one $K_I/\sigma\sqrt{\pi a} = 1.1215$, and it has an error of 0.062%

$$\begin{aligned} K_I/\sigma\sqrt{\pi a} &= 1.121 + 0.0159\beta - 0.221\beta^2 \\ K_{II}/\sigma\sqrt{\pi a} &= -0.684\beta \end{aligned} \tag{28}$$

In conclusion, the solution of SIFs at the crack tip for a bonded dissimilar semi-infinite plate takes the form

$$\begin{cases} K_I/\sigma\sqrt{\pi a} \to 0,\ K_{II}/\sigma\sqrt{\pi a} \to 0 \quad \text{when} \quad \alpha(\alpha-2\beta<0; \\ K_I/\sigma\sqrt{\pi a} = 1.121 + 0.0159\beta - 0.221\beta^2,\ K_{II}/\sigma\sqrt{\pi a} = -0.684\beta \\ \qquad\qquad \text{when} \quad \alpha(\alpha-2\beta) = 0; \\ K_I/\sigma\sqrt{\pi a} \to \infty,\ K_{II}/\sigma\sqrt{\pi a} \to \infty \quad \text{when} \quad \alpha(\alpha-2\beta > 0. \end{cases} \tag{29}$$

6.2. Stress intensity factors for a shallow edge interface crack in a bonded finite strip

In this section, the SIFs for the shallow edge interface cracks within the singular zone as shown in Fig. 12 are investigated using the improved proportional method. The results of $F_I \cdot (W/a)^{1-\lambda}$ and $F_{II} \cdot (W/a)^{1-\lambda}$ are plotted against logarithmic relative crack length a/W in Fig. 13(a) and (b), respectively. The material composite parameter β in Fig. 10 are restricted to $\beta = 0.3$, and similar phenomenon can be found from others material combinations of restricted β. As can be seen from these figures, the values for a given material combination approach a constant with more than 3-digit when $a/W < 10^{-2}$. Thus, we propose the following formula to calculate the SIFs at the crack tip for the shallow edge interface cracks in a bonded strip

$$\frac{K_I}{\sigma\sqrt{\pi a}} \cdot (a/W)^{1-\lambda} = C_I, \quad \frac{K_{II}}{\sigma\sqrt{\pi a}} \cdot (a/W)^{1-\lambda} = C_{II} \tag{30}$$

where C_I, C_{II} are constants depending upon the relative elastic properties of materials. The results for the coefficients C_I, C_{II} are plotted and listed against material composite parameters in Fig. 14(a) and Table 5 as well as in Fig. 14(b) and Table 6, respectively. The normalized SIFs F_I, F_{II} are often used to express the results of analysis.

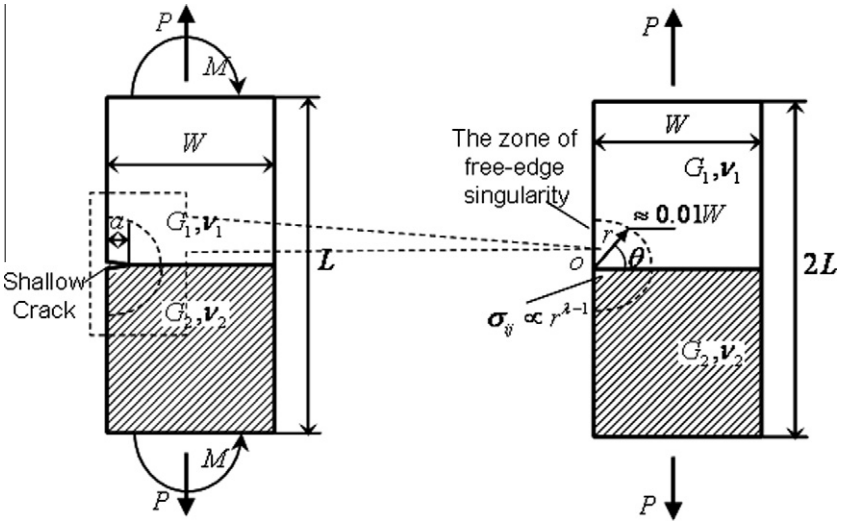

Fig. 12. Shallow edge interface crack in a bonded strip.

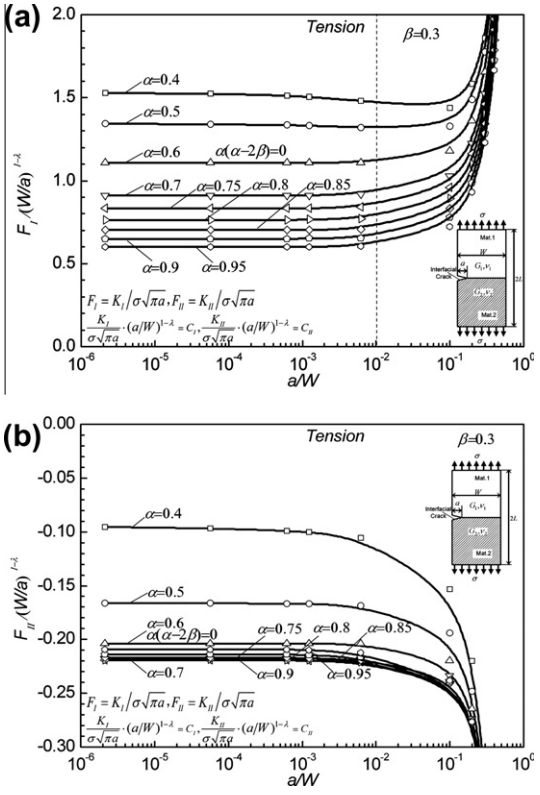

Fig. 13. The values of (a) $F_I \cdot (W/a)^{1-\lambda}$ and (b) $F_{II} \cdot (W/a)^{1-\lambda}$ for $\beta = 0.3$.

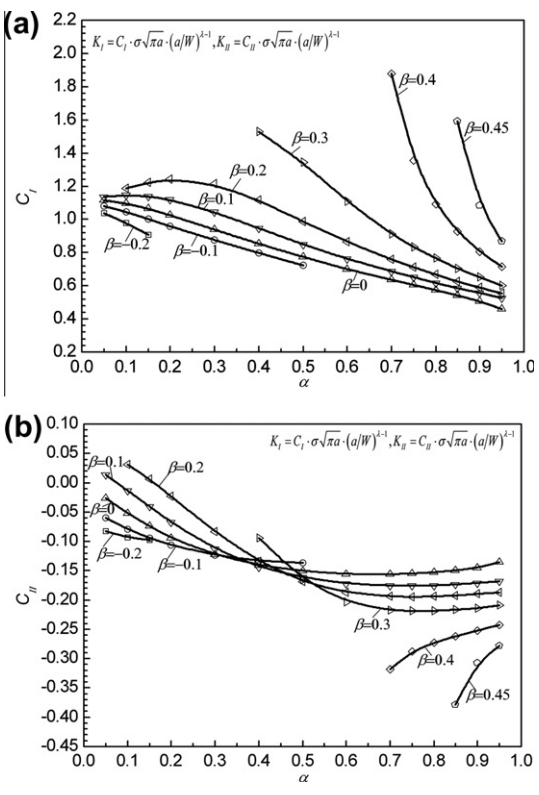

Fig. 14. Constants (a) C_I and (b) C_{II} for various combination of materials.

However, as indicated in Eq. (22), F_I, F_{II} are not suitable for edge interface cracks, because they sometimes go to infinity and sometimes approach zero as $a/W \to 0$. However, as indicated in Fig. 13, $C_I = F_I(W/a)^{1-\lambda}$, $C_{II} = F_{II}(W/a)^{1-\lambda}$ always have finite values when $a/W \to 0$. The reason can be explained from Fig. 10. In Fig. 10, $K_\sigma(\sigma W)^{1-\lambda}$ always have finite values although K_σ values themselves sometimes take infinite values and sometimes take zero.

From Figs. 10 and 14(a), it is seen that the coefficient curves C_I in Fig. 14(a) are similar to the intensities of singular stress of perfectly bonded strip in Fig. 10. This is because the SIFs for the shallow edge interface cracks are controlled by the singular zone at the interface corner for the perfectly bonded strip without crack as shown in Fig. 12.

7. Conclusions

In this paper an edge interface crack in a bonded strip were analyzed with varying the crack length and material combinations systematically. Then, the limiting solutions were provided in a bonded dissimilar semi-infinite plate subjected to remote uniform tension under arbitrary material combinations. To calculate the stress intensity factors, an exact solution for bonded infinite plate were

Table 5
Tabulated values of C_I.

α	$\beta=-0.2$	$\beta=-0.1$	$\beta=0$	$\beta=0.1$	$\beta=0.2$	$\beta=0.3$	$\beta=0.4$	$\beta=0.45$
0.05	1.036	1.082	1.114	1.136				
0.1	0.979	1.043	1.094	1.146	1.187			
0.15	0.907	1.001	1.063	1.14	1.221			
0.2		0.958	1.025	1.12	1.24			
0.3		0.875	0.938	1.044	1.215			
0.4		0.798	0.852	0.947	1.115	1.528		
0.5		0.721	0.772	0.85	0.986	1.343		
0.6			0.7	0.763	0.863	1.106		
0.7			0.635	0.686	0.756	0.912	1.876	
0.75			0.604	0.651	0.709	0.833	1.356	
0.8			0.573	0.618	0.666	0.764	1.092	
0.85			0.542	0.586	0.626	0.704	0.925	1.589
0.9			0.508	0.556	0.588	0.65	0.806	1.083
0.95			0.46	0.527	0.553	0.602	0.715	0.867

Table 6
Tabulated values of C_{II}.

α	$\beta=-0.2$	$\beta=-0.1$	$\beta=0$	$\beta=0.1$	$\beta=0.2$	$\beta=0.3$	$\beta=0.4$	$\beta=0.45$
0.05	−0.083	−0.06	−0.026	0.014				
0.1	−0.093	−0.079	−0.052	−0.013	0.031			
0.15	−0.098	−0.094	−0.074	−0.041	0.006			
0.2		−0.106	−0.094	−0.067	−0.023			
0.3		−0.124	−0.123	−0.113	−0.084			
0.4		−0.133	−0.141	−0.144	−0.135	−0.095		
0.5		−0.137	−0.151	−0.162	−0.169	−0.166		
0.6			−0.156	−0.172	−0.187	−0.204		
0.7			−0.156	−0.176	−0.194	−0.218	−0.318	
0.75			−0.155	−0.176	−0.195	−0.219	−0.288	
0.8			−0.153	−0.175	−0.194	−0.219	−0.273	
0.85			−0.15	−0.173	−0.193	−0.217	−0.262	−0.379
0.9			−0.145	−0.171	−0.19	−0.214	−0.252	−0.307
0.95			−0.136	−0.168	−0.187	−0.209	−0.243	−0.278

also considered to produce proportional singular stress fields by applying specific tensile and shear stresses at infinity. The details of this new numerical solution are described with clarifying the effect of the element size on the stress intensity factor.

1. The stress intensity factors are expressed for an edge crack in bonded semi-infinite plate in the following form

$$\begin{cases} K_1/\sigma\sqrt{\pi a},\quad K_2/\sigma\sqrt{\pi a}\to 0 \quad \text{when} \quad \alpha(\alpha-2\beta)<0 \\ K_1/\sigma\sqrt{\pi a}=1.121+0.0159\beta-0.221\beta^2 \\ K_2/\sigma\sqrt{\pi a}=-0.684\beta \quad \text{when} \quad \alpha(\alpha-2\beta)=0 \\ K_1/\sigma\sqrt{\pi a},\quad K_2/\sigma\sqrt{\pi a}\to\infty \quad \text{when} \quad \alpha(\alpha-2\beta)>0 \end{cases}$$

2. It is found that the stress intensity factors can be expressed in following forms if the edge interface crack is small enough within the zone of free-edge singularity of a bonded strip. Those coefficients C_1, C_2 are computed and tabulated under all material combinations in the $\alpha-\beta$ space

$$\frac{K_1}{\sigma\sqrt{\pi a}}\cdot(a/W)^{1-\lambda}=C_1,\quad \frac{K_2}{\sigma\sqrt{\pi a}}\cdot(a/W)^{1-\lambda}=C_2$$

3. The singular stress field for a bonded strip without crack is investigated under various material combinations because the SIFs for the small interface edge crack are controlled by this singular stress field.

Appendix. Dundurs' composite parameters for engineering materials

Till recently, several studies have considered the Dundurs' composite parameters of typical engineering materials. Suga et al. (1988) investigated the parameters and mechanical compatibility

Table A1
Elastic properties of several engineering materials (Yuuki, 1993).

Material		Young's modulus (GPa)	Poisson's ratio
Metal	Fe	206	0.30
	Al	70.3	0.345
	Ti	115.7	0.321
	Cu	129.8	0.343
	Zn	108.4	0.249
	Si	200	0.30
Ceramics	Al_2O_3	359	0.20
	SiC	440	0.16
	Si_3N_4	304	0.27
	MgO	303	0.175
Resin	Epoxy Resin	4.93	0.33
	Polyester	3.0	0.38
Glass	Crystal	73.1	0.17
	LF5	59.0	0.226
	SF53	58.0	0.236
	BaSF64	105.0	0.262
	BK7	81.5	0.208
	CaNa	70.3	0.240

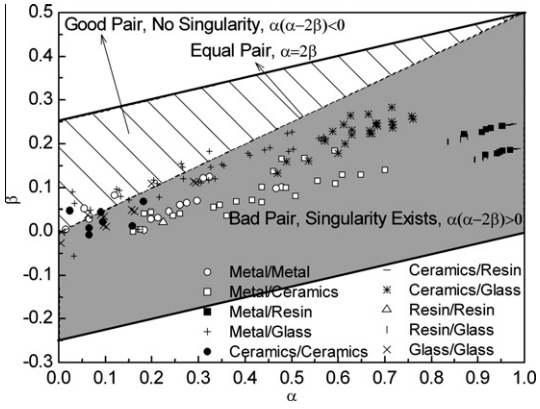

Fig. A1. Dundurs' composite parameters for several engineering materials.

of various material joints. Yuuki (1992) showed the variations of the parameters in the $\alpha-\beta$ space for the materials combinations among metal, ceramics, resin, and glass. The results are tabulated in Table A1 and re-plotted in Fig. A1. Consider the symmetry of $\alpha-\beta$ space for the bi-material joints, only the right part ($\alpha>0$) is given in Fig. A1. The origin $\alpha=\beta=0$ represents combinations of identical materials, and the $\alpha-\beta$ space is located within the parallelogram region which is composed by the lines $\beta=1/4(\alpha\pm1)$, $\alpha=0$, $\alpha=1$. Material combinations of $\alpha=2\beta$ are plotted in the dashed line. Uniform stress distributions can be observed for $\alpha=2\beta$. And the $\alpha-\beta$ space can be divided into two regions by the line $\alpha=2\beta$. Each pair of (α,β) above the line has no singularity and is denoted as good pair ($\alpha(\alpha-2\beta)<0$). And the one below the line is denoted as bad pair ($\alpha(\alpha-2\beta)>0$) since stress singularity exists near the interface corner.

As can been seen from Fig. A1, most material combinations are located in the so called "bad pair" region. However, metal-to-glass joints distribute along the line $\alpha=2\beta$, and a considerable number of metal-to-glass joints can be found in the "good pair" region. In addition, metal/metal, ceramics/ceramics and glass/glass joints are also found to have "good pair" material combinations.

References

Akisanya, A.R., Fleck, N.A., 1997. Interfacial cracking from the free edge of a long bimaterial strip. Int. J. Solids Struct. 34, 1645–1665.
Bogy, D.B., 1968. Edge-Bonded Dissimilar Orthogonal Elastic Wedges under Normal and Shear Loading. Trans ASME., J. Appl. Mech. 35, 460–466.

Bogy, D.B., 1971. Two edge-bonded elastic wedges of different materials and wedges angles under surface tractions. J. Appl. Mech. 38, 377–386.
Bogy, D.B., Wang, K.C., 1971. Stress singularities at interface corners in bonded dissimilar isotropic elastic materials. Int. J. Solids Struct. 7, 993–1005.
Chen, D.H., Nishitani, H., 1993. Intensity of singular stress field near the interface edge point of a bonded strip. Trans. JSME 59, 2682–2686 (in Japanese).
Dempsey, J.P., Sinclair, G.B., 1979. On the stress singularities in the plane elasticity of the composite wedge. J. Elasticity 9, 373–391.
Dong, Y.X., Wang, Z.M., Wang, B., 1997. On the computation of stress intensity factors for interfacial cracks using quarter point boundary elements. Eng. Fract. Mech. 57, 335–342.
Dundurs, J., 1969. Discussion of edge bonded dissimilar orthogonal elastic wedges under normal and shear loading. J. Appl. Mech. 36, 650–652.
Erdogan, F., 1965. Stress distribution in bonded dissimilar materials with cracks. Trans ASME., J. Appl. Mech. 2, 403–410.
Hein, V.L., Erdogan, F., 1971. Stress singularities in a two-material wedge. Int. J. Fract. Mech. 7, 317–330.
Ikeda, T., Soda, T., Munakata, T., 1993. Stress intensity factor analysis of interface crack using boundary element method – application of contour-integral method. Eng. Fract. Mech. 45, 599–610.
Liu, Y.H., Wu, Z., Liang, Y., Liu, X., 2008. Numerical methods for determination of stress intensity factors of singular stress field. Eng. Fract. Mech. 75, 4793–4803.
MSC Marc 2007 r1, 2007. MSC Marc 2007r1 User's Guide, 2007. MSC.Software Corp., California, USA.
Noda, N.A., Shirao, R., Li, J., Sugimoto, J.S., 2007. Intensity of singular stress fields causing interfacial de-bonding at the end of fiber under pull-out force and transverse tension. Int. J. Solids Struct. 44, 4472–4491.
Noda, N.A., Zhang, Y., Takaishi, K., Lan, X., 2010. Stress intensity factors of an interface crack in a bonded plate under uni-axial tension. J. Solid Mech. Mater. Eng. 4 (7), 974–987.
Oda, K., Kamisugi, K., Noda, N.A., 2009. Analysis of stress intensity factor for interface cracks based on proportional method. Trans. JSME 75, 476–482 (in Japanese).
Teranisi, T., Nisitani, H., 1999. Determination of highly accurate values of stress intensity factor in a plate of arbitrary form by FEM. Trans. JSME 65A, 16–21 (in Japanese).
Reedy Jr., E.D., Guess, T.R., 1993. Composite to metal tubular lap joints: strength and fatigue resistance. Int. J. Fract. 63, 351–367.
Suga, T., Elssner, G., Schmauder, S., 1988. Composite parameters and mechanical compatibility of material joints. J. Compos. Mater. 22, 917–934.
Van Vroonhoven, J.C.W., 1992. Stress singularities in bi-material wedges with adhesion and delamination. Fatigue Fract. Eng. Mater. Struct. 15, 157–171.
Williams, M.L., 1952. Stress singularities resulting from various boundary conditions in angular corners of plates in extension. J. Appl. Mech. 19, 526–528.
Wu, Y.L., 1996. A new method for evaluation of stress intensities for interface cracks. Eng. Fract. Mech. 48, 755–761.
Xu, J.Q., Liu, Y., Wang, X., 1999. Numerical methods for the determination of multiple stress singularities and related stress intensity coefficients. Eng. Fract. Mech. 63, 775–790.
Yang, X.X., Kuang, Z.B., 1996. Contour integral method for stress intensity factors of interface crack. Int. J. Fract. 78, 299–313.
Yuuki, R., Cho, S.B., 1989. Efficient boundary element analysis of stress intensity factors for interface cracks in dissimilar materials. Eng. Fract. Mech. 34, 179–188.
Yuuki, R., 1992. Mechanics of Interface, first ed. Baifuukann, Tokyo (in Japanese).
Zhang, Y., Noda, N.A., Takaishi, K., Lan, X., 2011. Stress intensity factors of a central interface crack in a bonded finite plate and periodic interface cracks under arbitrary material combinations. Eng. Fract. Mech. 78, 1218–1232.